

We are IntechOpen, the world's leading publisher of Open Access books Built by scientists, for scientists

6,900

Open access books available

186,000

International authors and editors

200M

Downloads

Our authors are among the

154

Countries delivered to

TOP 1%

most cited scientists

12.2%

Contributors from top 500 universities



WEB OF SCIENCE™

Selection of our books indexed in the Book Citation Index
in Web of Science™ Core Collection (BKCI)

Interested in publishing with us?
Contact book.department@intechopen.com

Numbers displayed above are based on latest data collected.
For more information visit www.intechopen.com



Investigation of the Gasoline Engine Performance and Emissions Working on Methanol-Gasoline Blends Using Engine Simulation

Simeon Iliev

Abstract

The aim of this study is to develop the one-dimensional model of a four-cylinder, four-stroke, multi-point injection system SI engine and a direct injection system SI engine for predicting the effect of various fuel types on engine performances, specific fuel consumption, and emissions. Commercial software AVL BOOST was used to examine the engine characteristics for different blends of methanol and gasoline (by volume: 5% methanol [M5], 10% methanol [M10], 20% methanol [M20], 30% methanol [M30], and 50% methanol [M50]). The methanol-gasoline fuel blend results were compared to those of net gasoline fuel. The obtained results show that when methanol-gasoline fuel blends were used, engine performance such as power and torque increases and the brake-specific fuel consumption increases with increasing methanol percentage in the blended fuel.

Keywords: methanol blends, alternative fuels, spark-ignition engine, emissions, engine simulation

1. Introduction

Alternative fuels are derived from resources other than petroleum. When using these fuels in internal combustion engines (ICE), they produce less air pollution emissions than gasoline. Most of them are more economically beneficial than fossil fuels. Last but not least, they are renewable. The most commonly used alternative fuels are natural gas, propane, methanol, ethanol, and hydrogen. Lots of works have been written on engine operating with these fuels individually, but very few compared some of these alternative fuels together in the same engine [1–3]. The idea of adding low contents of ethanol or methanol to gasoline is not new, extending back at least to the 1970s, when oil supplies were reduced and a search for alternative energy carriers began in order to replace gasoline and diesel fuel. Initially, methanol was considered the most attractive alcohol to be added to gasoline. Methanol production can be from biomass, coal, or natural gas with acceptable energy costs. The gasification of biomass can lead to methanol, mixed alcohols, and Fischer-Tropsch

liquids [4]. Since methanol can be produced from natural gas at no great cost, and is quite easy to blend with gasoline, this alcohol was seen as an attractive additive. Methanol can also be used in pure form in internal combustion engines; the fact that it is a liquid fuel makes it suitable for storing and distributing. It does produce hydrocarbon emissions similar to gasoline (different species); its single-carbon-molecule nature and combustion characteristics mean that its emissions of oxides of nitrogen and particulate matter are significantly lower than hydrocarbon fuels. However, when using methanol in practice, it became clear that precautions had to be taken when handling it and that methanol is aggressive to some materials, such as plastic components and even metals in the fuel system [5].

Methanol has many advantages (characteristics) that make it very suitable for use as a fuel in spark-ignition engine. Some of these characteristics are given in a **Table 1**, and they are as follows:

- High molar expansion ratio
- High hydrogen-to-carbon ratio
- Being liquid at standard temperature and pressure
- High heat of vaporization (“latent heat”)
- High flame speed
- Low combustion temperature
- High specific energy ratio (i.e., energy per unit of fuel-air mixture)

Methanol is the simplest alcohol and is usually referred to as the “light” alcohol. It is the simplest carbonaceous molecule that is liquid at standard temperature and pressure. This makes it easy to store and transport with minimal losses on the vehicle and in the fuel infrastructure. It is also known as methyl alcohol. The higher autoignition temperature of methanol compared to gasoline allows the engines to operate at a higher compression ratio; thereby they can be more efficient.

The methanol consists of just one molecule unlike gasoline, diesel, kerosene, etc. which the properties can change depending on the source, and as such it is easier to simulate the process for. The molecular weight of methanol is approximately four times lighter than gasoline. The diffusion rate of lighter fuel is lower than that of heavier fuel, and it results in lower emission.

Adding methanol to gasoline allows the fuel mixture to combust more completely due to the presence of oxygen (inherent oxygen in its molecular structure), which increases the combustion efficiency and reduces the emission of CO and NO_x by converting them into CO₂ and NO₂. Besides, methanol does not contain sulfur or complex organic compounds [9], resulting in zero emission of sulfur-based pollutants (SO₂ and SO₃, which are responsible for acid rain). The organic emissions (ozone precursors) from alcohol combustion have lower reactivity, which can stimulate ozone formation [10].

Methanol has a higher latent heat of vaporization than gasoline (**Table 1**). It provides a cooling effect on the intake charge compared to gasoline. This effect improves the brake thermal efficiency and power output. The lower caloric value of methanol due to oxygen content in its molecular structure requires higher fuel quantity to be injected in order to achieve an equivalent brake power output.

Properties	Gasoline	Methanol
Chemical formula	C ₈ H ₁₅	CH ₃ OH
Molar mass, kg/kmol	114	32
Oxygen content, wt%	—	50
Carbon content, wt%	86	38
Hydrogen content, wt%	14	12
Stoichiometric AFR	14,5	6,43
Lower heating value, MJ/kg	44,3	20,1
Higher heating value, MJ/kg	48	22,8
Volumetric energy content, MJ/m ³	31,746	15,871
Heat of evaporation, kJ/kg at 1 bar	375	1089
Research octane number	96,5	112
Motor octane number	87,2	91
Cetane number	—	<5
Boiling temperature, °C at 1 bar	27–245	65
Vapor pressure, bar at 20°C	0,25–0,45	0,13
Critical pressure, bar	—	81
Critical temperature, °C	—	239,4
Kinematic viscosity, cSt at 20°C	0,6	0,74
Destiny, kg/cm ³	740	798
Surface tension, N/m at 20°C	—	0,023
Minimum ignition energy, mJ at φ = 1	0,8	0,21
Autoignition temperature, °C	246–280	470
Peak flame temperature, °C at 1 bar	2030	1890
Adiabatic flame temperature, K	~ 2275	2143
Flammability limits (vol%)	1,4–7,6	6–36
Flash point, °C	–45	12
Bulk modulus, N/mm ² at 20°C 2 MPa	1300	823
Specific CO ₂ emissions, g/MJ	73,95	68,44
Specific CO ₂ emissions relative to gasoline	1	0,93

Table 1.
 Comparison of fuel properties [6–8].

The major issue encountered when blending water, methanol, and gasoline is phase separation. The critical phase separation temperature of methanol-gasoline blends increases with the amount of water present in the blend. Because of this very small water tolerance of the methanol-gasoline blend, water contamination during methanol transport and storage has to be avoided [11]. The blends with gasoline and low methanol concentrations will increase the vapor pressure.

Another important problem is related to the engine cold starting of very high blend alcohols in gasoline. Because of lower energy density and higher heat of vaporization of methanol, more mass needs to evaporate and therefore more energy. The lower flammability limit of methanol is higher than that of gasoline which is also the reason for cold starting [12].

Methanol has a higher octane number than pure gasoline fuel [13]. This enables higher compression ratios of engines and, as a result, increases its thermal efficiency [14].

There are many publications with different blends of alcohols and gasoline fuel. For example, Shenghua et al. [15] used a gasoline engine to examine different percentages of methanol blends (from 10 to 30%) in gasoline. From the results obtained, it has been established that power and engine torque decreased, whereas the brake thermal efficiency improved with the increase of methanol percentage in the fuel blend. Another study [16] has studied the influence of methanol-gasoline blends on the gasoline engine performance. The results obtained showed that the highest brake mean effective pressure (BMEP) was obtained from 5% methanol-gasoline blend. In another study, Altun et al. [17] studied the influence of methanol and ethanol blending (5 and 10%) in gasoline fuel on engine performance and emissions. Blended fuels showed the best result in emissions. The emissions of HC are reduced by 13 and 15% for E10 and M10. The results obtained show a decrease in CO emissions by 10,6 and 9,8%, but CO₂ emission increased for E10 and M10. The blended fuels with methanol and ethanol showed an increase in the brake-specific fuel consumption and a decrease in break thermal efficiency compared to gasoline. Some authors suggested that the oxygenated nature of alcohols can lead to more complete combustion and consequently to reduced engine-out CO emissions [18, 19]. Liang et al. [20] studied PM emission from gasoline direct-injected engine and port fuel-injected engine fueled by gasoline and methanol-gasoline blend M15. They found that the PM emission was lower for M15 than for gasoline.

2. Research methodology

The aim of the present chapter is to develop the one-dimensional model of four-stroke port fuel injection (PFI) gasoline engine and four-stroke direct injection (GDI) gasoline engine for predicting the effect of methanol-gasoline (M0–M50) addition to gasoline on the exhaust emissions and performance of gasoline engine. For this, simulation of gasoline SI engine (calibrated) as the basic operating condition and the laminar burning velocity correlations of methanol-gasoline blends for calculating the changed combustion duration were used. The engine power, specific fuel consumption, and exhaust emissions were compared and discussed [21, 22].

Computer simulation is becoming an important tool for time and cost efficiency in an engine's development. The simulation results are challenging to be obtained experimentally. Using computational fluid dynamics (CFD) has allowed researchers to understand the flow behavior and quantify important flow parameters such as mass flow rates or pressure drops, under the condition that the CFD tools have been properly validated against experimental results.

CFD software products include KIVA, AVL FIRE, AVSYS, STAR-CD, VECTIS, FLUENT, PHOENICS, Flow Vision, and more. The above programs allow to model with great accuracy the modeling of gases, the movement of the dispersed fuel in the combustion chamber of the engine, the movement of the thin layer of fuel formed on the surface of solid walls, the temperature field, and other phenomena. The fluid-structure interaction analysis, successfully implemented in the Ansys program, integrates state-of-the-art computational tools related to fluid and gas mechanics and solid-state mechanics to allow a multidisciplinary research.

The software for thermodynamic and gas-dynamic calculations include AVL BOOST, Ricardo WAVE, GT-Power, and others. These software products are characterized by a well-developed user interface that includes one-dimensional and multidimensional models.

2.1 Simulation setup

The simulation tools are the most used in recent years owing to its continuous increase in computational power. The use of engine simulations enables optimization of engine combustion, geometry, and operating characteristics toward improving specific fuel consumption and exhaust emissions and reducing engine development time and costs. Consequently, it can be expected that the use of engine simulations during engine construction will continue to increase. Engine modeling is a fruitful research area, and therefore many laboratories have their own engine thermodynamic models with varying degrees of complexity, scope, and ease of use [23].

Many researchers develop their own computer code describing different processes of engine operation. One of the studies [24] developed the computer code for simulating spark-ignited engine using alternative fuels, and results were validated with experimental data. The engine model is a quasi-dimensional two-zone model including ordinary differential equations for describing dynamical behavior during the intake, compression, power, and exhaust strokes. The engine model uses the Woschni correlation to estimate engine heat transfer. Another author [25] created a model for simulating the performance of spark-ignition engines fueled with gasoline and ethanol fuels and their mixtures. In this model the combustion chamber was divided into burned and unburned zones separated by a flame front. The pressure was assumed to be uniform throughout the cylinder charge. The instantaneous heat interaction between the burned and unburned zones and its walls was calculated by using the semiempirical expression for a four-stroke engine [26].

The one-dimensional engine simulation is widely used for design, development, calibration, and optimization because they make it possible for the entire engine to be modeled, they do not require high computing power, and the calculations are performed in a relatively short time [27, 28]. The one-dimensional (1D) engine model consists of sub-models of selected processes that can be investigated using more detailed modeling approaches (quasi-dimensional or three-dimensional models) to increase the accuracy of the overall engine simulation results.

The model of combustion as part of one-dimensional engine simulations provides the burning rate that represents the heat release rate in the combustion process for a given fuel blend, engine geometry, and set of operating conditions. The burning rate can be computed empirically and or derived from physical, detailed coupled turbulent flames, or chemical kinetic correlations of combustion processes.

The one-dimensional model of SI engine is created by the AVL BOOST software and has been employed to examine the emissions and performance working on gasoline and methanol-gasoline blends. The preprocessing steps of AVL BOOST enables the user to build a one-dimensional engine test bench setup using the predefined elements provided in the software toolbox. The various elements are joined by the desired connectors to establish the complete engine model using pipelines. It is important to make a correct estimate of the boundary conditions as it directly affects the accuracy of the results. Having a proper combustion model will enhance the understanding of the physical phenomena, including the effects of valve phasing, type of fuel, compression ratio, exhaust gas recirculation, etc., and, thus, enable comprehensive design and optimization of the engine.

In **Figure 1**, PFIE symbolizes the engine, while C1 to C4 are the cylinders of the SI engine. The cylinders of the engine are the main element in this model, because they have many very important parameters to settle: the bore, stroke, internal geometry, connecting rod, length and compression ratio, piston pin offset, and the mean crankcase pressure. MP1 to MP18 symbolize the measuring points. The plenum is market with PL1 to PL4. System boundary are market with SB1 and SB2. The

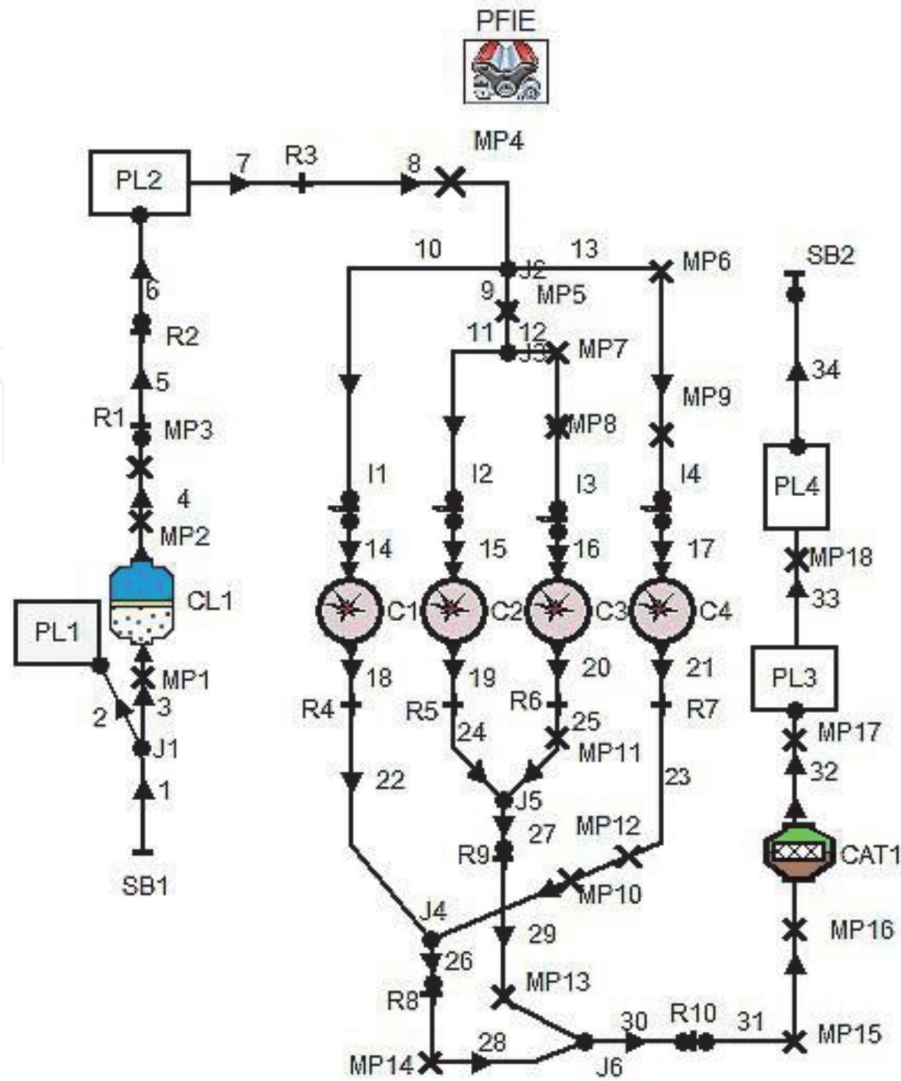


Figure 1.
Schematic of the gasoline PFI engine model.

cleaner is market with CL1. R1 to R10 stand for flow restrictions, CAT1 symbolize catalyst and fuel injectors—I1 to I4 are. The flow pipes are numbered 1 to 34.

The calibrated gasoline PFI engine model was described by Iliev [29], and its layout is shown in **Figure 1** with engine specification shown in **Table 2**.

The schematic of the calibrated GDI engine model is shown in **Figure 2** with engine specification shown in **Table 3**.

The comparison between the properties of gasoline and methanol is presented in **Table 1**. As shown in **Table 1**, compared with gasoline, methanol has a higher elemental oxygen content and a lower heating value, molecular weight, elemental carbon, hydrogen content and stoichiometric air/fuel ratio (AFR).

2.2 Description of combustion model

In this research, the Vibe (two-zone) model was chosen for simulation analysis of the combustion. The combustion chamber was divided into two regions: unburned gas region and burned gas regions [17]. For the burned charge and unburned charge, the first law of thermodynamics is applied:

$$\frac{dm_b u_b}{d\alpha} = -p_c \frac{dV_b}{d\alpha} + \frac{dQ_F}{d\alpha} - \sum \frac{dQ_{Wb}}{d\alpha} + h_u \frac{dm_b}{d\alpha} - h_{BB,b} \frac{dm_{BB,b}}{d\alpha} \quad (1)$$

Engine parameters	Value
Bore	86 (mm)
Stroke	86 (mm)
Compression ratio	10.5
Connection rod length	143.5 (mm)
Number of cylinders	4
Piston pin offset	0 (mm)
Displacement	2000 (cc)
Intake valve open	20 BTDC (deg)
Intake valve close	70 ABDC (deg)
Exhaust valve open	50 BBDC (deg)
Exhaust valve close	30 ATDC (deg)
Piston surface area	5809 (mm ²)
Cylinder surface area	7550 (mm ²)
Number of strokes	4

Table 2.
PFI engine specification.

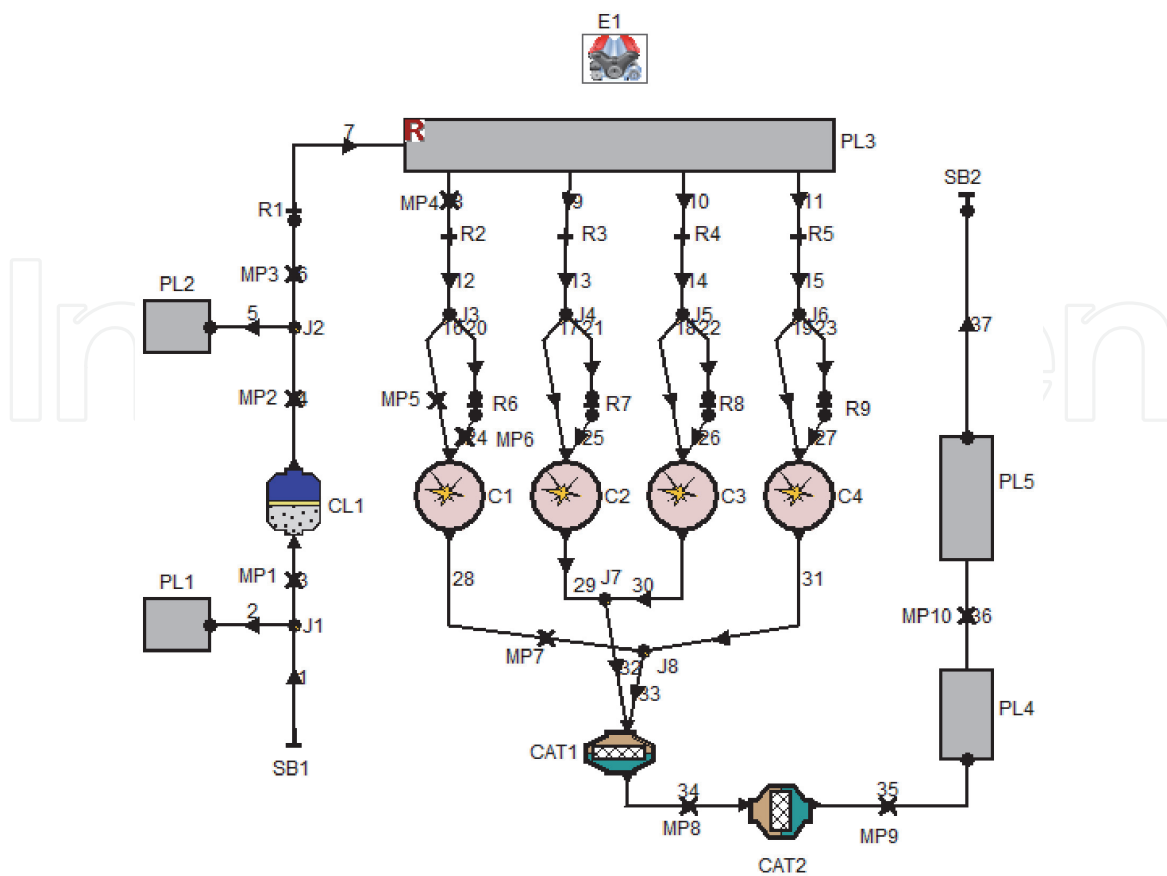


Figure 2.
Schematic of the gasoline GDI engine model.

Engine parameters	Value
Bore	80 (mm)
Stroke	78 (mm)
Compression ratio	11.9
Connection rod length	130 (mm)
Number of cylinders	4
Piston pin offset	0 (mm)
Displacement	1600 (cc)
Intake valve open	19 BTDC (deg)
Intake valve close	52 ABDC (deg)
Exhaust valve open	47 BBDC (deg)
Exhaust valve close	15 ATDC (deg)
Piston surface area	6600 (mm ²)
Cylinder surface area	7700 (mm ²)
Number of strokes	4

Table 3.
GDI engine specification.

$$\frac{dm_u u_u}{d\alpha} = -p_c \frac{dV_u}{d\alpha} - \sum \frac{dQ_{Wu}}{d\alpha} - h_u \frac{dm_B}{d\alpha} - h_{BB,u} \frac{dm_{BB,u}}{d\alpha} \quad (2)$$

where dm_u represents the change of the internal energy in the cylinder, $p_c \frac{dV}{d\alpha}$ is the piston work, $\frac{dQ_F}{d\alpha}$ stands for the fuel heat input, $\frac{dQ_W}{d\alpha}$ is wall heat losses, and $h_u \frac{dm_b}{d\alpha}$ represents the enthalpy flow from the unburned to the burned zone due to the conversion of a fresh charge to combustion products. The heat flux between the two zones is neglected. $h_{BB} \frac{dm_{BB}}{d\alpha}$ represents the enthalpy due to blow by, u and b in the subscript are unburned and burned gas.

Moreover, the sum of the zone volumes must be equal to the cylinder volume, and the sum of the volume changes must be equal to the cylinder volume change:

$$\frac{dV_b}{d\alpha} + \frac{dV_u}{d\alpha} = \frac{dV}{d\alpha} \quad (3)$$

$$V_b + V_u = V \quad (4)$$

The amount of burned mixture at each time setup is obtained from the Vibe function. For all other terms, for instance, wall heat losses, etc., models similar to the single zone models with an appropriate distribution on the two zones are used [30].

2.2.1 Mass fraction burned

The Wiebe function is widely used in internal combustion engine applications to describe the fraction of mass burned in the combustion chamber during the combustion process [31, 32].

To represent the mass fraction burned, the Wiebe function is chosen. The Wiebe function for mass fraction burned is shown by the equation below:

$$x_b = 1 - \exp \left[-a \left(\frac{\theta - \theta_o}{\Delta\theta} \right)^{m+1} \right] \quad (5)$$

where x_b is mass fraction burned, θ_o is start of combustion, $\Delta\theta$ is burn duration, a is efficiency factor, and b is shape factor (a and b are constant factors depending on the fuel). For this research, a complete combustion is assumed. The value of “ a ” is chosen to be 6.9 and the value of “ b ” to be 3 [33, 34]. The shape factor affects ignition delay and initial flame development. However, the values are subject to further analysis and provide scope for future research.

2.2.2 Mass fraction burned

The heat transfer to the walls of the combustion chamber is calculated from

$$Q_{wi} = hA_i(T_c - T_{wi}) \quad (6)$$

where Q_{wi} is wall heat flow, A_i is surface area, h is heat transfer coefficient, T_c is temperature of gas in the cylinder, and T_{wi} is wall temperature.

The Woschni model is selected to determine the heat transfer coefficient [35].

2.3 A description of exhaust emission model

In AVL BOOST the model of formation on NOx is based on Pattas and Hafner [30], which incorporates the Zeldovich mechanism [36]. The reaction of Zeldovich mechanism is given in **Table 4**.

The rate of NOx production was obtained using Eq. (7):

$$r_{NO} = C_{PPM}C_{KM}(2, 0) \cdot (1 - \alpha^2) \left(\frac{r_1}{1 + \alpha AK_2} + \frac{r_4}{1 + AK_4} \right) \quad (7)$$

$$\alpha = \frac{C_{NO.act}}{C_{NO.equ}} \cdot \frac{1}{C_{KM}} \quad (8)$$

$$AK_2 = \frac{r_1}{r_2 + r_3} \quad (9)$$

$$AK_4 = \frac{r_4}{r_5 + r_6} \quad (10)$$

In the above equation, C_{PPM} represents post-processing multiplier, C_{KM} denotes kinetic multiplier, C stands for molar concentration in equilibrium, and r_i represents reactions rates of the Zeldovich mechanism.

	Stoichiometry	Rate $k_i = k_{0,i} T^a e^{\left(\frac{-T_{A_i}}{T}\right)}$	K_0 (cm ³ /mol s)	a [-]	T_A [K]
R1	$N_2 + O = NO + N$	$r_1 = k_1 c_{N_2} c_O$	4.93E13	0.0472	38,048,01
R2	$O_2 + N = NO + O$	$r_2 = k_2 c_{O_2} c_N$	1.48E08	1.5	2859,01
R3	$N + OH = NO + H$	$r_3 = k_3 c_{OH} c_N$	4.22E13	0.0	0,0
R4	$N_2O + O = NO + NO$	$r_4 = k_4 c_{N_2O} c_O$	4.58E13	0.0	12,130,6
R5	$O_2 + N_2 = N_2O + O$	$r_5 = k_5 c_{O_2} c_{N_2}$	2.25E10	0.825	50,569,7
R6	$OH + N_2 = N_2O + H$	$r_6 = k_6 c_{OH} c_{N_2}$	9.14E07	1.148	36,190,66

Table 4.
 Reactions according to the Zeldovich mechanism.

The model of NO_x formation is based on Onorati et al. [37]:

$$r_{CO} = C_{Const}(r_1 + r_2).(1 - \alpha) \quad (11)$$

$$\alpha = \frac{C_{CO.act}}{C_{CO.equ}} \quad (12)$$

In Eq. (11), C represents molar concentration in equilibrium and r_i represents reaction rates based on the model.

The unburned HC have different sources. A complete description of HC formation still cannot be given, and the achievement of a reliable model within a thermodynamic approach is definitely prevented by the fundamental assumptions and the requirement of reduced computational times. Still, a phenomenological model which accounts for the main formation mechanisms and is able to capture the HC trends as function of the engine operating parameter may be proposed. The following important sources of unburned HC can be identified in SI engines [38]:

1. During the intake and compression stroke, fuel vapor is absorbed into the oil layer and deposits on the cylinder walls. The following desorption occurs when the cylinder pressure decreases during the expansion stroke, and complete combustion cannot take place anymore.
2. A fraction of the charge enters the crevice volumes and is not burned since the flame quenches at the entrance.
3. Occasional complete misfire or partial burning takes place when combustion quality is poor.
4. Quench layers on the combustion chamber wall which are left as the flame extinguishes prior to reaching the walls.
5. The flow of fuel vapor into the exhaust system during valve overlap in gasoline engines.

The first two mechanisms and in particular the crevice formation are considered to be the most important and need to be accounted for in a thermodynamic model. Partial burn and quench layer effect cannot be physically described in a quasi-dimensional approach, but may be included by adopting tunable semiempirical correlations.

The formation of unburned HC in the crevices is described by assuming that the pressure in the cylinder and in the crevices is the same and that the temperature of the mass in the crevice volumes is equal to the piston temperature.

The mass in the crevices at any time is described by Eq. (13):

$$m_{crevice} = \frac{pV_{crevice}M}{RT_{piston}} \quad (13)$$

In Eq. (13), $m_{crevice}$ represents the mass of unburned charge in the crevice, p denotes cylinder pressure, $V_{crevice}$ stands for total crevice volume, M represents unburned molecular weight, T_{piston} is the temperature of the piston, and R denotes gas constant.

The second important source of HC is the presence of lubricating oil in the fuel or on the walls of the combustion chamber. During the compression stroke, the fuel vapor pressure increases, so, by Henry's law, absorption occurs even if the oil was saturated during the intake. During combustion the concentration of fuel vapor in

the burned gases goes to zero, so the absorbed fuel vapor will desorb from the liquid oil into the burned gases. Fuel solubility is a positive function of the molecular weight, so the oil layer contributed to HC emissions depending on the different solubilities of individual hydrocarbons in the lubricating oil.

The assumptions made in the development of the HC absorption/desorption are the following:

1. Fuel is constituted by a single hydrocarbon species, completely vaporized in the fresh mixture.
2. The oil film temperature is at the same as the cylinder wall.
3. Traverse flow across the oil film is negligible.
4. Oil is represented by squalane (C₃₀H₆₂), whose characteristics resemble those of the SAE5W20 lubricant.
5. Diffusion of the fuel in the oil film is the limiting factor, for the diffusion constant in the liquid phase is 104 times smaller than the corresponding value in the gas phase.

The radial distribution of the fuel mass fraction in the oil film can be determined by solving the diffusion Eq. (14):

$$\frac{\partial w_F}{\partial t} - D \frac{\partial^2 w_F}{\partial r^2} = 0 \quad (14)$$

In Eq. (14), w_F represents fuel's mass fraction in the oil film, t is the time, r stands for radial position in the oil film (distance from the wall), and D is relative (fuel-oil) diffusion coefficient.

3. Result and discussion for gasoline PFI engine

The present research focused on the performance and emission characteristics of the methanol-gasoline blends. Various concentrations of the blends 0% methanol (M0), 5% methanol (M5), 10% methanol (M10), 20% methanol (M20), 30% methanol (M30), 50% methanol (M50), and 85% methanol (M85) by volume were analyzed.

3.1 Engine performance characteristics

Figures 3 and 4 show the results of the brake power and torque for methanol-gasoline blended fuels at various engine speeds.

The variation of brake power versus engine speed was obtained at full load conditions for various concentrations of M5, M10, M20, M30, M50, and net gasoline M0. When the methanol content in the blended fuel was increased (M10, M20 and M30), the brake power slightly increased for all engine speeds. The brake power at net gasoline was higher in comparison of M50 for all engine speeds. The methanol's heat of evaporation is higher than that of gasoline fuel, providing air-fuel charge cooling and increasing the density of the charge. The methanol's blended fuel causes the equivalence ratio of blend approaches to stoichiometric condition which can lead to a better combustion. However, methanol's heating value is lower

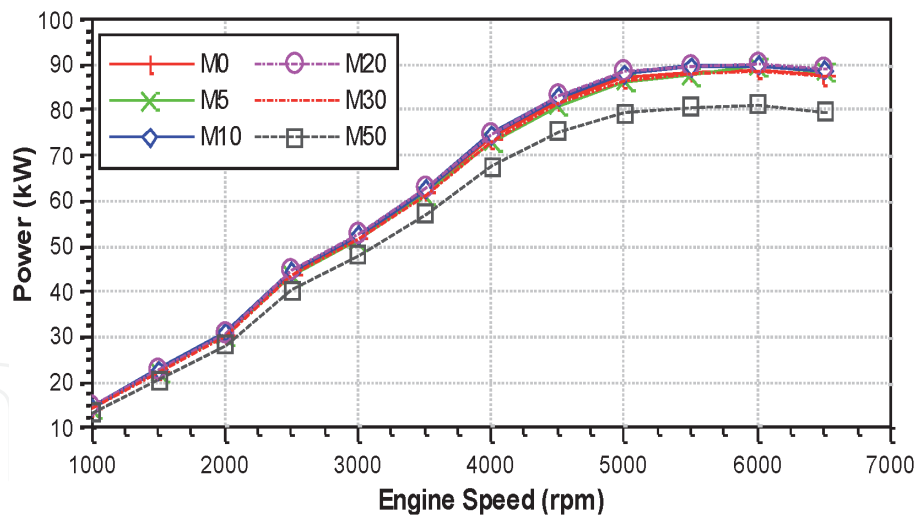


Figure 3.
Influence of methanol-gasoline blended fuels on brake power.

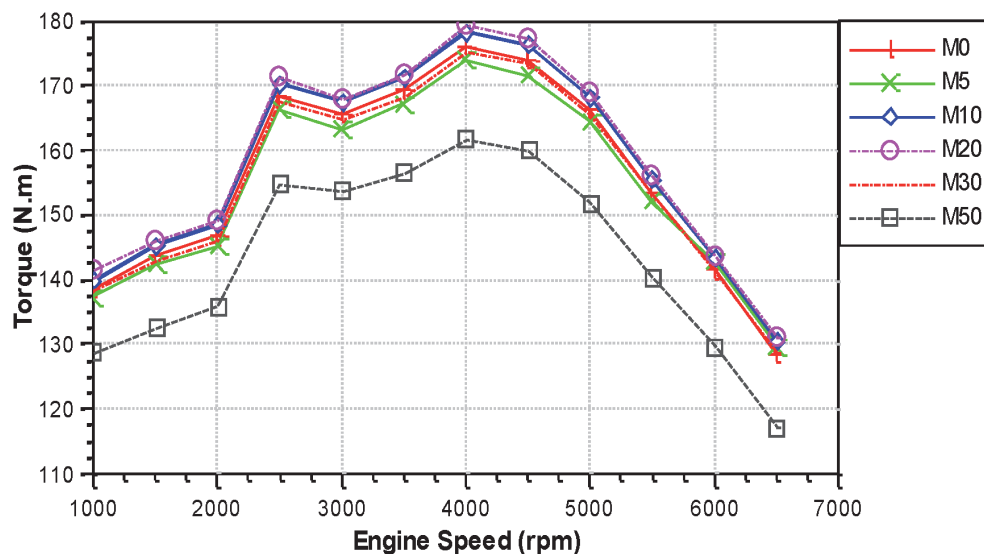


Figure 4.
Influence of methanol-gasoline blended fuels on engine torque.

than that of gasoline, and it can neutralize the previous positive effects. Consequently, a lower power output is obtained at M50.

Figure 4 shows the engine torque for various percentages of methanol in its blends with gasoline. Increasing the methanol content (M10 and M20) increased slightly the torque of the engine. The brake torque of gasoline was higher than those of M30 and M50.

Because of the existence of oxygen in the methanol chemical component, and the increase of methanol, lean mixtures are produced that decrease the equivalent air-fuel ratio to a lower value, and due to the presence of oxygen in the combustion chamber, the burning is more efficient.

Figure 5 shows the BSFC for various percentages of methanol in its blends with gasoline versus engine speeds. As shown in this figure, the BSFC increased as the methanol percentage increased. The reason has been known—the heating value and stoichiometric air-fuel ratio are the smallest for this fuel, which means that more fuel is needed for specific air-fuel equivalence ratio. The highest specific fuel consumption is obtained at M50 blended fuel.

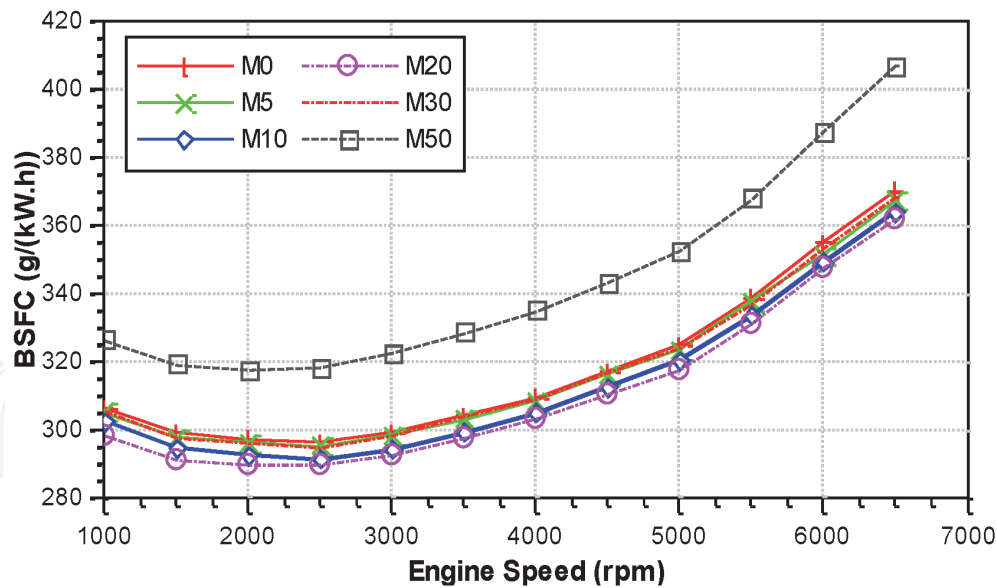


Figure 5.
 Influence of methanol-gasoline blended fuels on brake-specific fuel consumption.

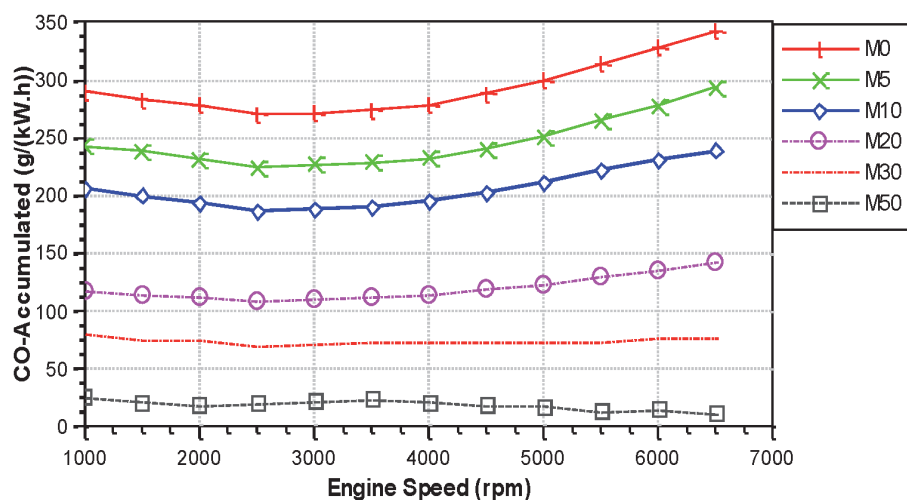


Figure 6.
 Influence of methanol-gasoline blended fuels on CO emissions.

Furthermore, there is a small difference between the BSFC for net gasoline and the mixtures with methanol (M5 to M30). As engine speed increased reaching 2000 rpm, the BSFC decreased reaching its minimum value.

3.2 Emission characteristics

The effect of the methanol-gasoline blends on CO emissions versus engine speeds can be seen in **Figure 6**. When methanol percentage increases, the CO emissions decrease. The reason for this could be explained with the enrichment of oxygen owing to the methanol, in which an increase in the proportion of oxygen will promote the further oxidation of CO during the engine exhaust process. Another significant reason for this reduction is that methanol (CH_3OH) has less carbon than gasoline (C_8H_{18}).

The effect of the methanol-gasoline blends on HC emissions is shown in **Figure 7**. When methanol percentage increases, the HC concentration decreases. The HC emissions decrease with the increase of the relative air-fuel ratio.

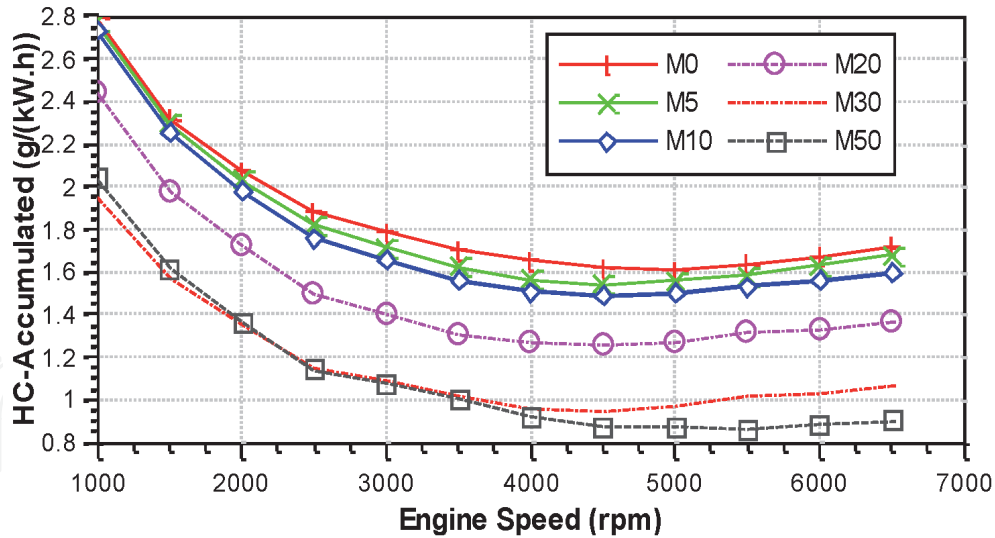


Figure 7. Influence of methanol-gasoline blended fuels on HC emissions.

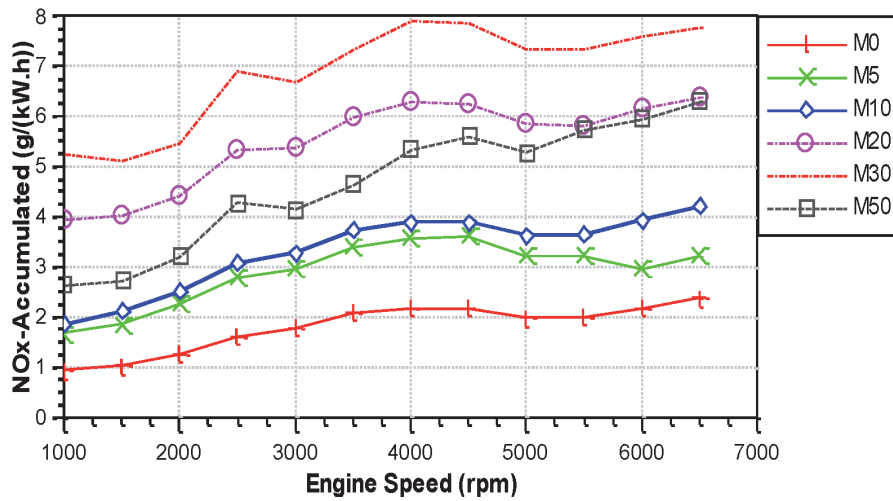


Figure 8. Influence of methanol-gasoline blended fuels on NOx emissions.

The influence of the methanol-gasoline blends on NOx emissions can be seen in **Figure 8**. The methanol-gasoline blends lead to an increase in NOx emissions as compared to the net gasoline. When combustion process is closer to stoichiometric, flame temperature increases, and the NOx emissions increase as well.

4. Result and discussion for gasoline GDI engine

Different concentrations of the blends (0% methanol (M0), 5% methanol (M5), 10% methanol (M10), 20% methanol (M20), 30% methanol (M30), and 50% methanol (M50) by volume) were analyzed using AVL BOOST at full load conditions for GDI engine.

4.1 Engine performance characteristics

The results of the brake power and specific fuel consumption for methanol-gasoline blended fuels at different engine speeds are shown in **Figures 9 and 10**.

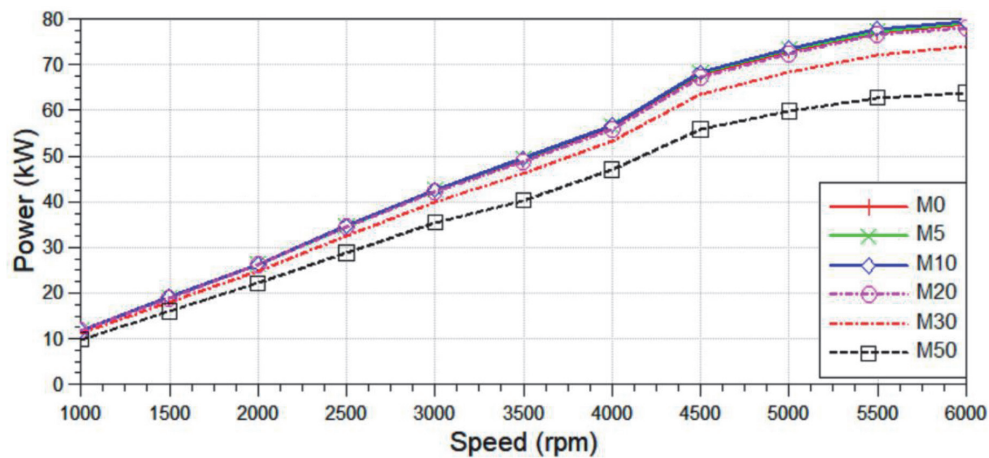


Figure 9.
 Influence of methanol-gasoline blended fuels on brake power.

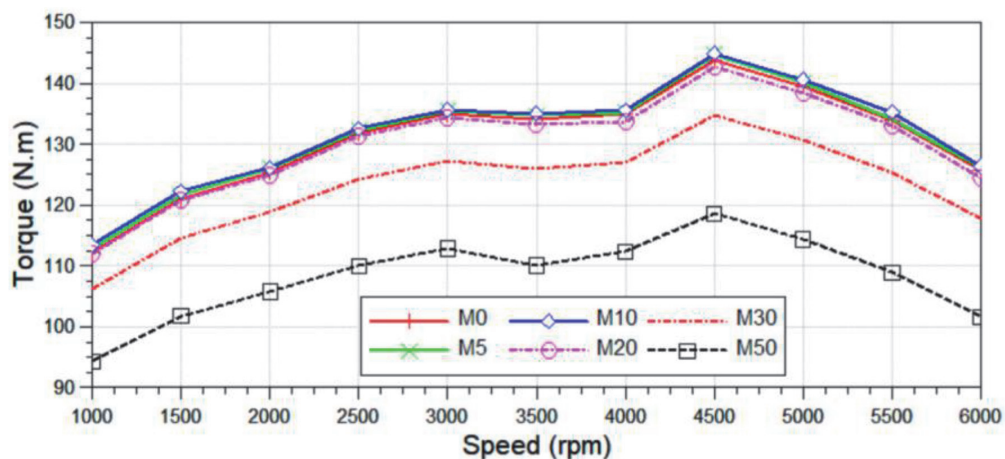


Figure 10.
 Influence of methanol-gasoline blended fuels on engine torque.

The variation of brake power versus engine speed was obtained at full load conditions for various concentrations of M5, M10, M20, M30, M50, and net gasoline M0. When the methanol content in the blended fuel was increased (M5 and M10), there was not a significant increase in engine brake power. The engine brake power was higher in operation with gasoline in comparison to M50 for all engine speeds. The methanol's heat of evaporation is higher than that of gasoline fuel, providing air-fuel charge cooling and increasing the density of the charge. The methanol blended fuel causes the equivalence ratio of blend approaches to stoichiometric condition which can lead to a better combustion. However, methanol's heating value is lower than that of gasoline, and it can neutralize the previous positive effects. Consequently, a lower power output is obtained at M50.

Figure 10 shows the engine torque for various percentages of methanol in its blends with gasoline. Increasing methanol content (M5 and M10) increased slightly the torque of the engine. The brake torque of gasoline was higher than those of M20, M30, and M50.

Because of the existence of oxygen in the methanol chemical component, and the increase of methanol, lean mixtures are produced that decrease the equivalent air-fuel ratio to a lower value, and due to the presence of oxygen in the combustion chamber, the burning is more efficient.

Figure 11 shows BSFC for various percentages of methanol in its blends with gasoline versus engine speeds. As shown in this figure, the BSFC increased as the

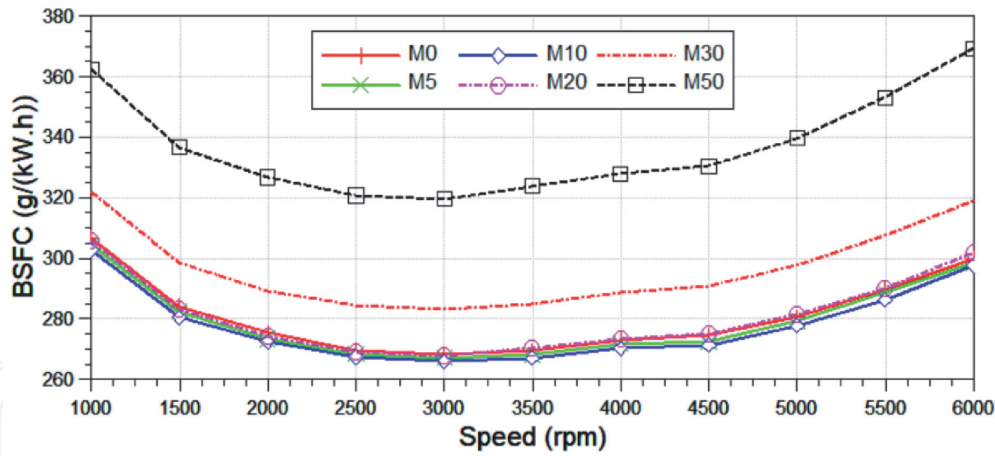


Figure 11.
Influence of methanol-gasoline blended fuels on brake-specific fuel consumption.

methanol percentage increased. This can be described with heating value and stoichiometric air-fuel ratio are the smallest for these two fuels, which means that for specific air-fuel equivalence ratio more fuel is needed. The highest specific fuel consumption is obtained at M50 blended fuel.

Furthermore, there is a small difference between the BSFC for net gasoline and the mixtures with methanol (M5 to M20). As engine speed increased reaching 3000 rpm, the BSFC decreased, reaching its minimum value.

4.2 Emission characteristics

The effect of the methanol-gasoline blends on CO emissions versus engine speeds can be seen in **Figure 12**. When methanol percentage increases, the CO emissions decrease. The reason for this could be explained with the enrichment of oxygen owing to the methanol, in which an increase in the proportion of oxygen will promote the further oxidation of CO during the engine exhaust process. Another significant reason for this reduction is that methanol (CH_3OH) has less carbon than gasoline (C_8H_{18}). Typical of direct injection engines is that they work with lean mixtures. Ensuring sufficient oxygen in the piston bowl for good flame

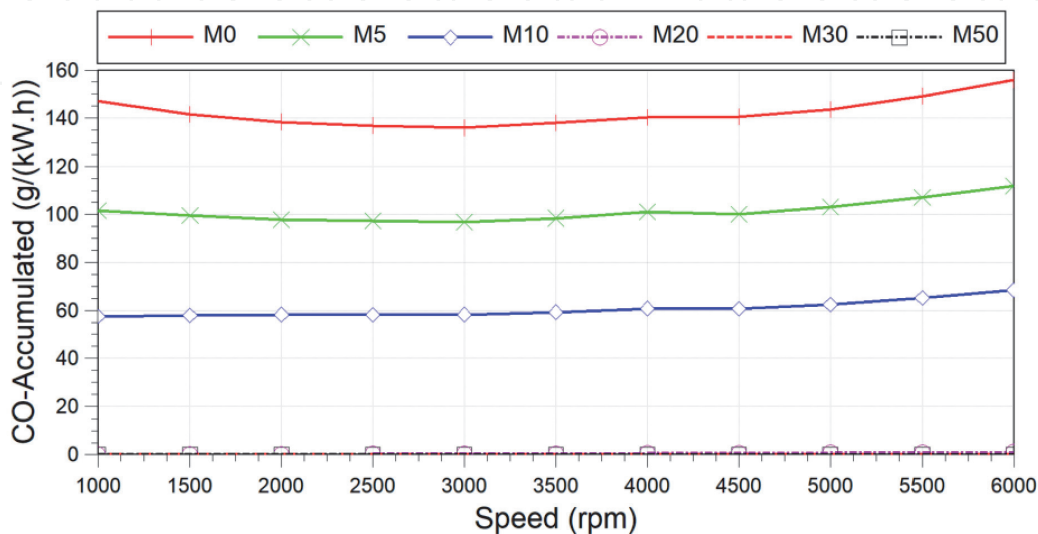


Figure 12.
Influence of methanol-gasoline blended fuels on CO emissions.

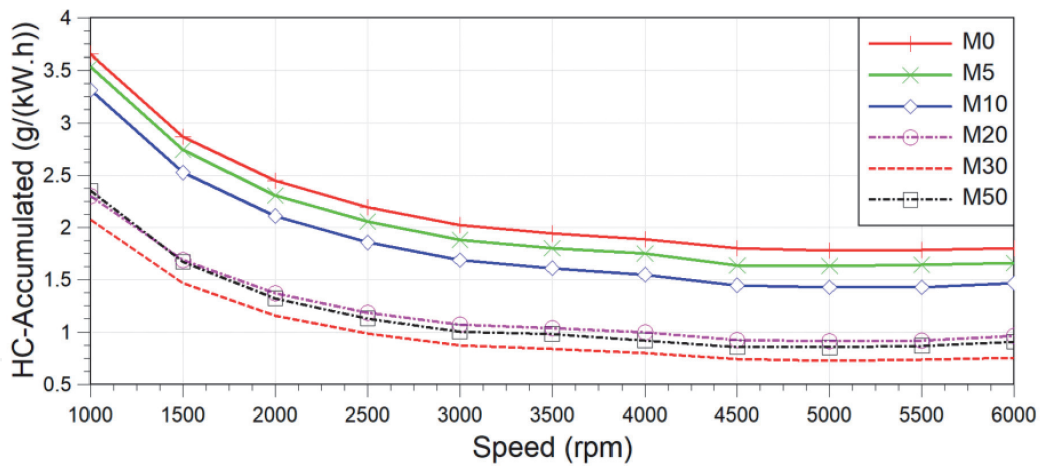


Figure 13.
Influence of methanol-gasoline blended fuels on HC emissions.

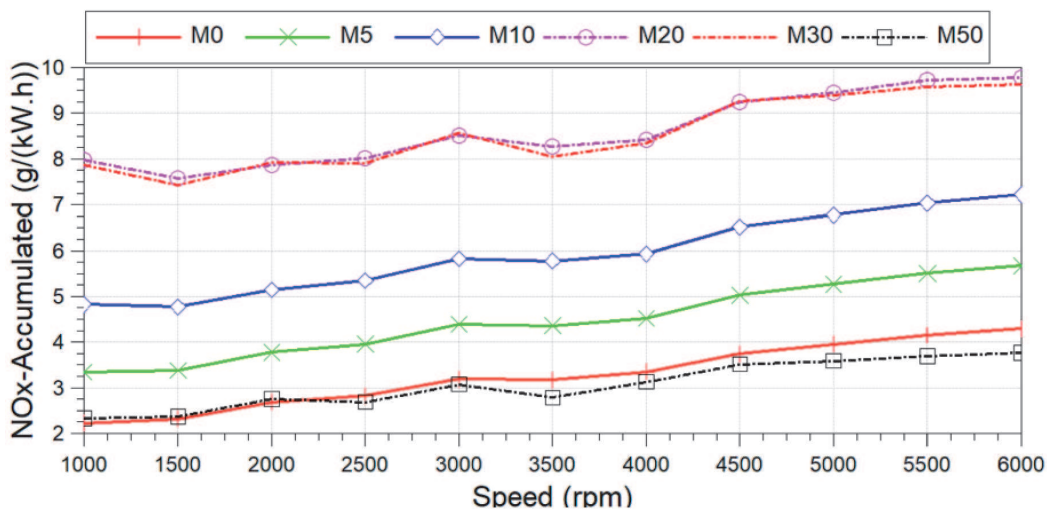


Figure 14.
Influence of methanol-gasoline blended fuels on NOx emissions.

propagation leads to higher combustion efficiency, reduced CO emissions, and optimal burn duration.

The influence of the methanol-gasoline blends on HC emissions is visible in **Figure 13**. When methanol percentage increases, the HC concentration decreases. The HC emissions decrease with the increase of the relative air-fuel ratio.

The effect of the methanol-gasoline blends on NOx emissions can be seen in **Figure 14**. When methanol percentage increases, the NOx concentration increases. Other authors [39] have obtained similar results. When combustion process is closer to stoichiometric, flame temperature increases, and the NOx emissions increase as well. The higher combustion temperature and local oxygen concentration in the peak temperature zone were the influencing factors for NOx emission formation.

5. Conclusions

The purpose of the present chapter is to demonstrate the influences of methanol addition to gasoline on a four-cylinder, four-stroke, multipoint injection system SI engine and a direct injection system SI on engine performance and emission characteristics. The summarized results from this study are the following.

With the increase of the percentage of methanol in the blended fuel, the engine brake power decreased for various engine speeds for PFI engine and GDI engine.

With the increase of the percentage of methanol in the blends (M5 to M10 for PFI engine and M5 to M10 for GDI engine), the brake power slightly increased, and with the increase of the methanol in the blends (M30 and M50), the brake power decreased.

As the percentage of methanol increased, the BSFC increased. The blended fuels show lower engine brake power and higher BSFC than net gasoline. Furthermore, there is a slight difference between the BSFC of gasoline and gasoline blended fuels (M10 and M20 for PFI engine and M5 and M10 for GDI engine).

When there is an increase in methanol percentage, the CO and HC concentration decreases for PFI and GDI engines.

Increasing the percentage of methanol in the blends leads to a significant increase in NO_x emissions. The lowest NO_x emissions are obtained at M50 methanol-gasoline blend at GDI engines.

Acknowledgements

The present chapter has been written with the Project No 2020-RU-03's financial assistance.

We are also eternally grateful to AVL-AST, Graz, Austria, for granting the use of AVL BOOST under the university partnership program.

IntechOpen

Author details

Simeon Iliev
University of Ruse "Angel Kanchev", Ruse, Bulgaria

*Address all correspondence to: spi@uni-ruse

IntechOpen

© 2020 The Author(s). Licensee IntechOpen. This chapter is distributed under the terms of the Creative Commons Attribution License (<http://creativecommons.org/licenses/by/3.0>), which permits unrestricted use, distribution, and reproduction in any medium, provided the original work is properly cited. 

References

- [1] Iliev S. Investigation of N-butanol blending with gasoline using a 1-D engine model. Proceedings of the 3rd International Conference on Vehicle Technology and Intelligent Transport Systems (VEHITS 2017). 2017:385-391. DOI: 10.5220/0006284703850391
- [2] Pourkhesalian AM, Shamekhi AH, Salimi F. Alternative fuel and gasoline in an SI engine: A comparative study of performance and emissions characteristics. *Fuel*. 2010;**89**:1056-1063
- [3] Varol Y, Oner C, Oztop HF, Altun S. Comparison of methanol, ethanol, or n-butanol blending with unleaded gasoline on exhaust emissions of an SI engine. *Energy Source, Part A*. 2014;**36**:938-948
- [4] Chum H, Overend R. Biomass and renewable fuels. *Fuel Processing Technology*. 2001;**71**:187-195. DOI: 10.1016/S0378-3820(01)00146-1
- [5] Egebäck K, Henke M, Rehnlund B, Wallin M, Westerholm R. Blending of ethanol in gasoline for spark ignition engines—Problem inventory and evaporative measurements. *Rapport MTC*. 2005;**5407**:8-9
- [6] MAN Diesel & Turbo. Using Methanol Fuel in the MAN B&W ME-LGI Series, 5510-0172-00ppr; 2014
- [7] Iliev S. Comparison of Ethanol and Methanol Blending with Gasoline Using Engine Simulation, Biofuels—Challenges and Opportunities. Mansour Al Qubeissi: IntechOpen; 2018. pp. 139-159. DOI: 10.5772/intechopen.81776
- [8] Vancoillie J. Modeling the Combustion of Light Alcohols in Spark-Ignition Engines. Vakgroep Mechanica van Stroming, Warmte en Verbranding Sint-Pietersnieuwstraat 41, B-9000 Gent, België: Ghent University; 2013. pp. 45-47
- [9] Elfasakhany A. Investigation on performance and emissions characteristics of an internal combustion engine fueled with petroleum gasoline and a hybrid methanol-gasoline fuel. *IJET-IJENS*. 2013;**13**:24-43
- [10] Akutsu Y, Toyoda F, Tomita K, Yoshizawa F, Tamura M, Yoshida T. Effect of exhaust from alcohol fuel on ozone formation in the atmosphere. *Atmospheric Environment: Part A General Top*. 1991:1383-1389. DOI: 10.1016/0960-1686(91)90247-5
- [11] Liu D, Qi Q, Zhang H, et al. Properties, performance, and emissions of methanol-gasoline blends in a spark ignition engine. Proceedings of the Institution of Mechanical Engineers, Part D. 2005;**219**(3):405-412
- [12] Pearson RJ, Turner JWG. GEM ternary blends: Testing iso-stoichiometric mixtures of gasoline, ethanol and methanol in a production flex-fuel vehicle fitted with a physical alcohol sensor. SAE Paper No. 2012-01-1279; 2012
- [13] Silva R, Cataluna R, Menezes EW, Samios D, Piatnicki CMS. Effect of additives on the antiknock properties and Reid vapor pressure of gasoline. *Fuel*. 2005;**84**:951-959
- [14] Raveendran K, Ganesh A. Heating value of biomass and biomass pyrolysis products. *Fuel*. 1996;**75**:1715-1720
- [15] Shenghua L, Clemente ERC, Tiegang H, Yanjv W. Study of spark ignition engine fueled with methanol/gasoline fuel blends. *Applied Thermal Engineering*. 2007;**27**:1904-1910
- [16] Bilgin A, Sezer I. Effects of methanol addition to gasoline on the performance and fuel cost of a spark ignition engine. *Energy & Fuels*. 2008;**22**:2782-2788

- [17] Altun S, Oztop H, Oner C, Varol Y. Exhaust emissions of methanol and ethanol-unleaded gasoline blends in a spark ignition engine. *Thermal Science*. 2013;17(1):291-297
- [18] Liu SH, Clemente ERC, Hu TG, et al. Study of spark ignition engine fueled with methanol/gasoline fuel blends. *Applied Thermal Engineering*. 2007;27(11-12):1904-1910. DOI: 10.1016/j.applthermaleng.2006.12.024
- [19] Svensson E, Li C, Shamun S et al. Potential levels of soot, NO_x, HC and CO for methanol combustion. SAE Technical Paper 2016-01-0887; 2016
- [20] Liang B, Ge Y, Tan J, Han X, Gao L, Hao L, et al. Comparison of PM emissions from a gasoline direct injected (GDI) vehicle and a port fuel injected (PFI) vehicle measured by electrical low pressure impactor (ELPI) with two fuels: Gasoline and M15 methanol gasoline. *Journal of Aerosol Science*. 2013;57:22-31
- [21] Iliev S. A comparison of ethanol and methanol blending with gasoline using a 1-D engine model. *Procedia Engineering*. 2015;100:1013-1022. DOI: 10.1016/j.proeng.2015.01.461
- [22] Iliev S. A comparison of ethanol, methanol and butanol blending with gasoline and relationship with Engine performances and emissions. In: *Proceedings of the 29th DAAAM International Symposium*; 2018. pp. 0505-0514
- [23] Alla GA. Computer simulation of a four stroke spark ignition engine. *Energy Conversion and Management*. 2012;43(8):1043-1061
- [24] Pourkhesalian AM, Shamekhi AH, Salimi F. Alternative fuel and gasoline in an si engine: A comparative study of performance and emissions characteristics. *Fuel*. 2010;89(5): 1056-1063
- [25] Al-Baghdadi MAS. A simulation model for a single cylinder four-stroke spark ignition engine fueled with alternative fuels. *Turkish Journal of Engineering and Environmental Sciences*. 2007;30(6):331-350
- [26] Gatowski J, Balles EN, Chun K, Nelson F, Ekchian J, Heywood JB. Heat Release Analysis of Engine Pressure Data, Technical Report. Warrendale, PA: Society of Automotive Engineers, Inc.; 1984
- [27] Heywood JB. Engine combustion modeling—An overview. In: Mattavi JN, Amann CA, editors. *Combustion Modeling in Reciprocating Engines*. New York: Plenum Press; 1980. pp. 1-35. ISBN 0-306-40431-1
- [28] Heywood JB. *Internal Combustion Engine Fundamentals*. New York: McGrawHill; 1988
- [29] Iliev S, Hadjiev K. Theoretical study of engine performance working on methanol-gasoline blends. *Proceedings of the WCE*. 2014;II:1459-1463
- [30] AVL List GmbH. *AVL Boost—Theory*. Hans-List-Platz 1, A-8020 Graz, Austria; 2013
- [31] Heywood JB et al. Development and use of a cycle simulation to predict SI engine efficiency and NO_x emissions. SAE. 1979;790291
- [32] Montenegro G, Onorati A, Piscaglia F, D'Errico G. Integrated 1D-multi-D fluid dynamic models for the simulation of ICE intake and exhaust systems. SAE Technical Paper Series 2007. pp. 3-7. Technical Report 2007-01-0495; 2007. DOI: 10.4271/2007-01-0495
- [33] Ghojel J. Review of the development and applications of the Wiebe function: A tribute to the contribution of Ivan Wiebe to engine research. *International*

Journal of Engine Research. 2010;**11**(4):
297-312

[34] Agarwal AK, Karare H, Dhar A. Combustion, performance, emissions and particulate characterization of a methanol-gasoline blend (gasohol) fuelled medium duty spark ignition transportation engine. Fuel Processing Technology. 2014;**121**:16-24

[35] Woschni G. A Universally Applicable Equation for the Instantaneous Heat Transfer Coefficient in the Internal Combustion Engine, Technical Report; SAE Technical Paper; 1967

[36] Bowman C. Kinetics of pollutant formation and destruction in combustion. Progress in Energy and Combustion Science. 1975;**1**(1):33-45

[37] Onorati A, Ferrari G, D'Errico G. 1D unsteady flows with chemical reactions in the exhaust duct-system of S.I. engines: Predictions and Experiments. SAE Paper No. 2001-01-0939. 2001

[38] Montenegro G, Onorati A. Modeling of silencers for IC engine intake and exhaust systems by means of an integrated 1D-multiD approach. SAE International Journal of Engines. 2009; **1**(1):466. DOI: 10.4271/2008-01-0677

[39] Gong Li Y, Deng YW, Yuan WH, Fu J, Zhang B. Experimental comparative study on combustion, performance and emissions characteristics of methanol, ethanol and butanol in a spark ignition engine. Applied Thermal Engineering. 2017;**115**: 53-63. DOI: 10.1016/j.applthermaleng.2016.12.037